AAC Journals.ASM.org

Assessment of Antiviral Properties of Peramivir against H7N9 Avian Influenza Virus in an Experimental Mouse Model

Amber Farooqui,[a,b,c] Linxi Huang,[d] Suwu Wu,[e] Yingmu Cai,[f] Min Su,[g] Pengzhou Lin,[d] Weihong Chen,[e] Xibin Fang,[e] Li Zhang,[a] Yisu Liu,[a] Tiansheng Zeng,[a] Stephane G. Paquette,[b,h] Adnan Khan,[a,c] Alyson A. Kelvin,[b] David J. Kelvin[a,b,c,h,i]

Division of Immunology, International Institute of Infection and Immunity, University Health Network & Shantou University Medical College, Shantou, China[a]; Division of Experimental Therapeutics, Toronto General Hospital Research Institute, University Health Network, Toronto, Ontario, Canada[b]; Guangdong Provincial Key Laboratory of Infectious Diseases and Molecular Immunopathology, Shantou, Guangdong, China[c]; Infectious Diseases Department, The First Affiliated Hospital of Shantou University Medical College, Shantou, China[d]; Intensive Care Unit, Shantou Central Hospital, Shantou, China[e]; Department of Laboratory Medicine, The First Affiliated Hospital of Shantou University Medical College, Shantou, Guangdong, China[f]; Department of Pathology, Shantou University Medical College, Shantou, China[g]; Institute of Medical Science, Faculty of Medicine, University of Toronto, Toronto, Ontario, Canada[h]; Department of Immunology, Faculty of Medicine, University of Toronto, Toronto, Ontario, Canada[i]

The H7N9 influenza virus causes a severe form of disease in humans. Neuraminidase inhibitors, including oral oseltamivir and injectable peramivir, are the first choices of antiviral treatment for such cases; however, the clinical efficacy of these drugs is questionable. Animal experimental models are essential for understanding the viral replication kinetics under the selective pressure of antiviral agents. This study demonstrates the antiviral activity of peramivir in a mouse model of H7N9 avian influenza virus infection. The data show that repeated administration of peramivir at 30 mg/kg of body weight successfully eradicated the virus from the respiratory tract and extrapulmonary tissues during the acute response, prevented clinical signs of the disease, including neuropathy, and eventually protected mice against lethal H7N9 influenza virus infection. Early treatment with peramivir was found to be associated with better disease outcomes.

The H7N9 influenza virus is a novel avian-origin influenza virus that emerged in February 2013 (1). Since then, the virus has sustained its presence, as sporadic human cases are seen throughout the year, with the largest numbers typically appearing in winters, following the trend of seasonal flu viruses (2, 3). Unlike lowly pathogenic influenza viruses, the H7N9 virus causes severe human illness, characterized by a pneumonia that rapidly develops into acute respiratory distress syndrome (ARDS), multiple-organ dysfunction (MOD), and shock (4). To date, 619 human cases have been reported from 16 different territories or provinces in mainland China (5, 6), while a few cases in patients with a recent history of travel to China also appeared, in Hong Kong (6), Taiwan (7), Malaysia, and Canada (8). Among these cases, nearly 70% of patients required intensive care support and mechanical ventilation, and approximately 34% died (9). Scientific evidence about limited airborne transmission among ferrets (10) as well as the appearance of family clusters could not rule out the possibility of human-to-human transmission and raises serious global concern (11).

Due to intrinsic adamantane resistance, H7N9 influenza virus infections are treated primarily with neuraminidase inhibitors (NAIs), particularly oseltamivir and, to some extent, intravenous administration of peramivir or zanamivir (9). Clinical data have demonstrated that the emergence of NA-R292K variants that encode NAI resistance in a few H7N9 cases during oseltamivir therapy had effects on viral eradication and resulted in high respiratory viral loads (12). These mutants also developed NAI resistance when tested in cells, but without an effect on replication and infectivity (13). Despite the fact that most H7N9-infected strains are sensitive to oseltamivir in cell culture, high mortality rates have been documented for H7N9-infected patients receiving oseltamivir therapy (14–16). This demonstrates the critical need to evaluate all available antiviral options.

Peramivir is an intravenous (i.v.) NAI prescribed by the National Health and Family Planning Commission for the treatment of severe H7N9 cases (17). It is a distant sialic acid analogue (a cyclopentane derivative with a guanidino group and lipophilic side chain) that shares structural features with both zanamivir and oseltamivir and similarly targets influenza virus neuraminidase activity. Limited clinical data are available for patient compliance with this drug, and so far it has not been evaluated in experimental animal models of H7N9 influenza virus infection. *In vitro* studies showed that peramivir has antiviral activity comparable to that of oseltamivir against H7N9 viruses (18, 19); however, the rapid bioavailability of the drug through the intravenous route might have an added advantage in treating patients with ARDS and MOD. In H7N9 cases, the drug is typically administered as a follow-up to oseltamivir, at which point the virus may have accumulated mutations that confer resistance to both drugs. Peramivir has previously been used for severe pandemic H1N1- or H5N1-infected

Received 3 August 2015 **Returned for modification** 28 August 2015
Accepted 3 September 2015

Accepted manuscript posted online 14 September 2015

Citation Farooqui A, Huang L, Wu S, Cai Y, Su M, Lin P, Chen W, Fang X, Zhang L, Liu Y, Zeng T, Paquette SG, Khan A, Kelvin AA, Kelvin DJ. 2015. Assessment of antiviral properties of peramivir against H7N9 avian influenza virus in an experimental mouse model. Antimicrob Agents Chemother 59:7255–7264. doi:10.1128/AAC.01885-15.

Address correspondence to David J. Kelvin, dkelvin@jidc.org.

Supplemental material for this article may be found at http://dx.doi.org/10.1128/AAC.01885-15.

patients in Japan, the United States, and other parts of the world, with recommended dosages of 300 to 600 mg i.v. daily for 5 days, or until the end of viral shedding in respiratory specimens in the case of immunocompromised patients (20–23).

Given the evidence of resistance to oseltamivir among circulating H7N9 viruses (24), we sought to evaluate the antiviral efficacy of peramivir *in vivo* and to ascertain its suitability as a front-line therapeutic for the treatment of H7N9. Here we report on the antiviral activity of peramivir in H7N9-infected C57/BL6 mice.

MATERIALS AND METHODS

Isolation of H7N9 influenza virus. The influenza virus A/Shantou/1001/2014 (H7N9) was isolated from a lung aspirate collected from a patient with a fatal case of influenza, reported from The First Affiliated Hospital of Shantou University Medical College, Guangdong Province, China, in March 2014 and confirmed to be an H7N9 infection by the Chinese Center of Disease Control and Prevention. The whole-genome sequence of the virus was already deposited in GISAID's EpiFlu database, under identifier EPI_Isl_162618, and has already been reported (25). The virus was cultivated, propagated, and titrated in 9- to 10-day-old embryonated chicken eggs for 72 h at 37°C. The hemagglutination test was performed using 1% horse red blood cells (RBCs) as described by the WHO. Virus isolation and infection procedures were performed in animal biosafety level 3 containment facilities, and the ethical committee of The First Affiliated Hospital of Shantou University Medical College approved the study.

Cells and compound. Madin-Darby canine kidney (MDCK) cells were obtained from ATCC, China. Cells were maintained in Dulbecco's modified Eagle's medium (DMEM) (Gibco, Beijing, China) supplemented with 10% heat-inactivated fetal bovine serum (FBS), 100 U penicillin, 100 μg/ml streptomycin, and 100 mM L-glutamine. Peramivir was purchased from Biocryst Pharmaceutical, Shanghai, China, and a stock solution was prepared in 0.85% NaCl and stored at −80°C.

Animal infection and treatment procedures. Six- to 8-week-old female C57/BL6 mice (Vital River, Beijing, China) were maintained on standard feed and water in a specific-pathogen-free (SPF) facility with controlled environmental temperature and humidity.

For this study, several sets of experiments were performed. The following protocols were used in each experiment; each group consisted of 16 mice. The animals were anesthetized by intraperitoneal (i.p.) administration of 2,2,2-tribromoethanol (Sigma, Steinheim, Germany) prior to inoculation and experimental procedures. For survival experiments, 10 animals from each group were monitored for clinical signs, weight loss, and mortality for up to 14 days postinfection (dpi). More than 20% loss of the original body weight was considered the humane endpoint for this study. Animals were specifically monitored for any neurological symptoms throughout the disease course.

For the characterization of viral pathogenicity, animals were divided into four different groups ($n = 16$) and inoculated intranasally (i.n.) with 50 μl of A/Shantou/1001/2014 (H7N9) virus inoculum containing 10^3, 10^4, 10^5, or 10^6 50% egg infective doses (EID_{50}) of viral particles.

To assess antiviral activity *in vivo*, we administered peramivir to animals infected i.n. with different concentrations of A/Shantou/1001/2014 (H7N9) virus, such as 10^3, 10^4, 10^5, and 10^6 EID_{50}. Briefly, 30 mg peramivir/kg body weight was administered to the thigh muscles in a final volume of 50 μl for each mouse. The treatment was given once daily from the time of infection until 8 dpi. An equal amount of 0.85% NaCl was administered in the same manner to vehicle groups.

In dose-dependent experiments, peramivir at 30, 15, and 3 mg/kg was administered to animals ($n = 16$/group) as described above. The treatment was given once daily from the time of infection until 8 dpi. The animals were infected with 10^4 EID_{50} of A/Shantou/1001/2014 (H7N9) virus i.n.

We next evaluated four different treatment regimens in mice infected with 10^4 EID_{50} of A/Shantou/1001/2014 (H7N9) virus. In the first two groups, a single dose of 30 mg/kg of peramivir was administered to mice ($n = 16$/group) immediately (single dose D0) or 24 h after inoculation (single dose D1). The next two groups were given multiple doses of peramivir, initiated at the day of infection or 1 day later. The groups were designated "multiple doses D0-D8" and "multiple doses D1-D8," respectively.

Estimation of viral loads in body tissues. At 3 and 6 dpi, animals from treated and untreated groups ($n = 3$/group) were euthanized, and body tissues, such as the lungs, liver, intestine, spleen, kidneys, stomach, lymph nodes, heart, and brain, were removed aseptically and rinsed in phosphate-buffered saline (PBS). Lung tissues were homogenized in 1 ml PBS, and homogenates were titrated in MDCK cells by a 50% tissue culture infective dose ($TCID_{50}$) assay according to the Reed and Muench method. Viral RNAs were extracted from other tissues by using a viral RNA minikit (Qiagen, Hilden, Germany) and converted into cDNAs by using a high-capacity cDNA RT kit (Life Technologies, Foster City, CA). The cDNAs were then subjected to quantitative real-time PCR (qRT-PCR) using influenza virus M gene-specific primers. qRT-PCR was performed with SYBR green qPCR supermix (Invitrogen, Carlsbad, CA) on a MyiQ real-time PCR detection system (Bio-Rad, Hercules, CA). Results are expressed as viral copy numbers per milliliter.

Histology and immunostaining. Tissues were collected at 3 and 6 dpi from treated and untreated groups and were also removed from surviving animals (after euthanization) from the peramivir treatment group, fixed with 4% buffered formalin, processed, and embedded in paraffin. Tissue sections were stained with hematoxylin and eosin (H&E). Viral staining was performed using an anti-influenza virus nucleoprotein (NP) antibody (Bio X Cell, West Lebanon, NH).

Statistical analyses. Statistical analysis was performed by using GraphPad Prism 6 software (GraphPad Inc.). Student's *t* test and one-way analysis of variance (ANOVA) were applied for comparisons of two and more than two groups, respectively. Survival curves were analyzed by the log rank test. *P* values of <0.05 were considered significant.

RESULTS

Characterization of A/Shantou/1001/2014 (H7N9) virus in C57/BL6 mice. We first characterized the pathogenicity of H7N9 influenza virus in C57/BL6 mice. Animals exhibited severe weight loss and lethal disease following infection with 10^4, 10^5, and 10^6 EID_{50} of H7N9 virus. The median number of days to death was 7 for the dose of 10^4, 4.5 for the dose of 10^5, and 4 for the dose of 10^6. Animals infected with 10^3 EID_{50} gradually lost body weight from 6 dpi, had a delayed time of death, and had a 70% mortality rate (Fig. 1a and b). Clinical signs included minimal physical activity, hunched posture, lethargy, and ruffled fur and started to appear in infected animals starting at 3 dpi. The virus was detected in lung tissues at levels as high as 7.7 $\log_{10}$ $TCID_{50}$/ml at 3 dpi and 5.9 $\log_{10}$ $TCID_{50}$/ml at 6 dpi, whereas viral spread to other body organs, such as the brain, intestine, liver, spleen, stomach, kidneys, and heart, was found at 3 dpi (data not shown).

Histology of lung sections revealed that lethal challenge (10^4 and 10^5 EID_{50}) with H7N9 influenza virus induced interstitial pneumonia and a marked inflammatory response in lungs. At 3 dpi, pathology was typically characterized by an infiltration of neutrophils and mononuclear cells and the presence of multiple focalized lesions—intense in the periphery—and hemorrhaging. Pulmonary exudates were predominantly present in the bronchial lumen, and the disappearance of nuclei from the bronchial epithelium, suggesting bronchial necrosis, was also observed (Fig. 2A to D). At 6 dpi, the lesions were similar, but with a predominant presence of lymphoid structures and involvement of the larger portions of the lungs. A typical lobular pneumonia that almost destroyed the lung architecture was observed, combined with heavy infiltration of mononuclear cells in the bronchial lumen

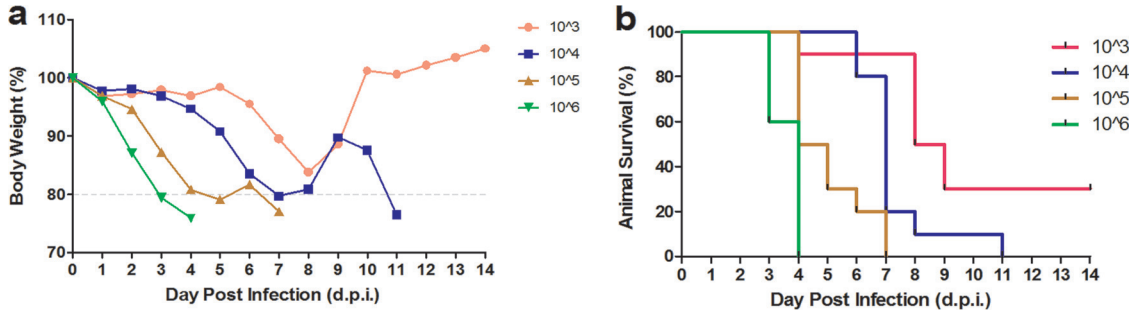

FIG 1 Pathogenicity of A/Shantou/1001/2014 H7N9 influenza virus in C57/BL6 mice. Animals ($n = 10$/group) were infected with different viral concentrations by the intranasal route, and weight loads (a) and mortality (b) were monitored until 14 dpi. Survival curves were found to be significantly different at each viral concentration ($P < 0.0005$).

and peribronchial spaces and around blood vessels. Signs of bronchial spasm were also seen in heavily inflamed spaces. Emphysema was observed at the lung periphery (Fig. 2E to H).

Effect of peramivir on the outcome of H7N9 influenza disease. We assessed the antiviral activity of peramivir in C57/BL6 mice challenged with different viral concentrations representing high (10^5 and 10^4) and low (10^3) infective doses. Intramuscular injection of 30 mg/kg of peramivir was performed on mice once daily from the day of infection to 8 dpi, while normal saline (0.85% NaCl) was administered in the same manner to the vehicle group. Peramivir treatment saved all animals in the 10^3 dose group, compared to 70% lethality in the vehicle (untreated) group ($P < 0.0005$). Furthermore, these animals did not exhibit any clinical signs and weight loss during the course of infection (Fig. 3a and b). Peramivir treatment also prevented death in 80% and 20% of animals challenged with 10^4 and 10^5 EID_{50} of H7N9 virus. In the 10^4 dose group, weight loss was observed only from 7 to 9 dpi, with the maximal dip at 8 dpi, which is significantly different from the case for the vehicle group ($P < 0.001$). Milder clinical signs, such as lethargy, dyspnea, and grouping, were also observed during this period. Peramivir treatment significantly lowered the risk of death ($P < 0.0001$), and the animals were able to recover toward the end of the disease course (Fig. 3c and d). Although only a 20% survival benefit was noticed in heavily infected (10^5) animals after peramivir treatment, these animals exhibited significant differences ($P < 0.001$) in weight loss from 4 to 7 dpi, extending the median survival time from 4.5 to 8 dpi compared to the vehicle group (Fig. 3e and f).

In agreement with the survival curve, peramivir treatment also led to dramatic reductions in lung virus titers regardless of the viral infection dose. A >4-log_{10} reduction was observed in the 10^3 and 10^4 dose groups, with a >2-log_{10} reduction in the 10^5 dose group, at 3 dpi ($P < 0.0001$). Complete viral eradication was seen in the 10^3 dose group at 6 dpi, with a >4-log_{10} reduction in viral replication in the other groups at the same time point ($P < 0.0001$) (Fig. 3g and h). Peramivir treatment also reduced the viral load in extrapulmonary tissues (see Appendix SA1 in the supplemental material). Even though decreased viral replication and a

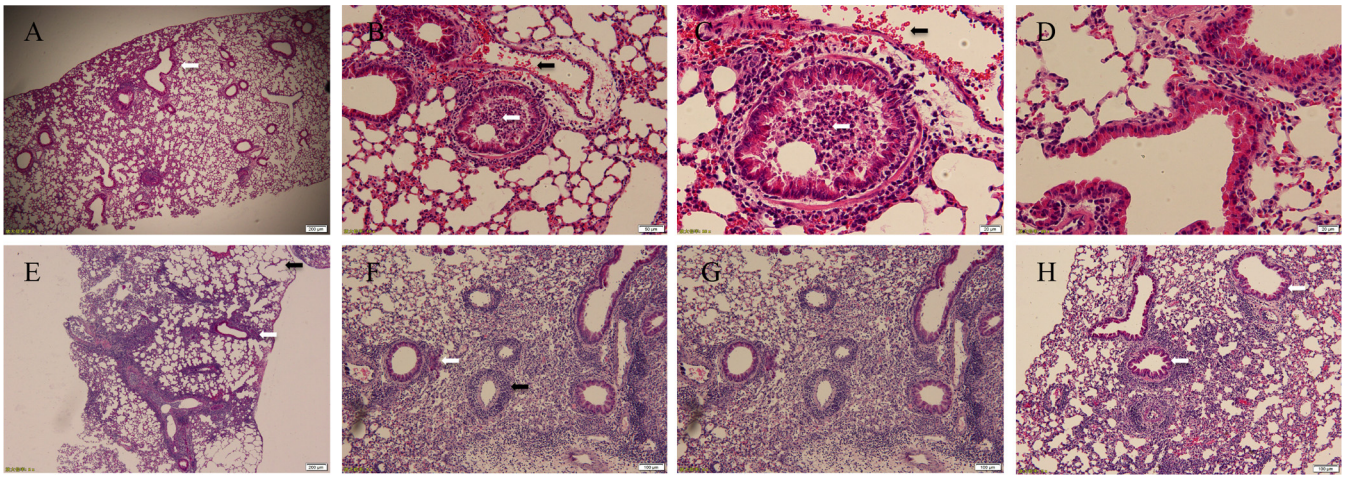

FIG 2 Pathological changes in lung tissues infected with A/Shantou/1001/2014 H7N9 influenza virus. C57/BL6 mice were infected with 10^4 EID_{50} of H7N9 virus, and lung sections were stained with H&E. Lung sections at 3 dpi showed interstitial pneumonia with focalized lesions at the periphery (white arrow) (original magnification, ×40) (A), hemorrhage (black arrows), the presence of pulmonary exudates, and infiltration of neutrophils and mononuclear cells into the bronchial lumen (white arrows) (original magnifications, ×100 and ×200) (B and C), and bronchial necrosis (original magnification, ×200) (D). Tissue inflammation was intense at 6 dpi, with the involvement of larger portions, the presence of lymphoid structures (white arrows), and signs of emphysema (black arrow) (original magnification, ×40) (E), heavy infiltration of inflammatory cells, specifically lymphocytes, in peribronchial (white arrow) and perivascular (black arrow) areas (original magnification, ×40) (F), typical lobular pneumonia resulting in diffused alveolar damage (original magnification, ×100) (G), and signs of bronchial spasm (white arrows) (original magnification, ×100) (H).

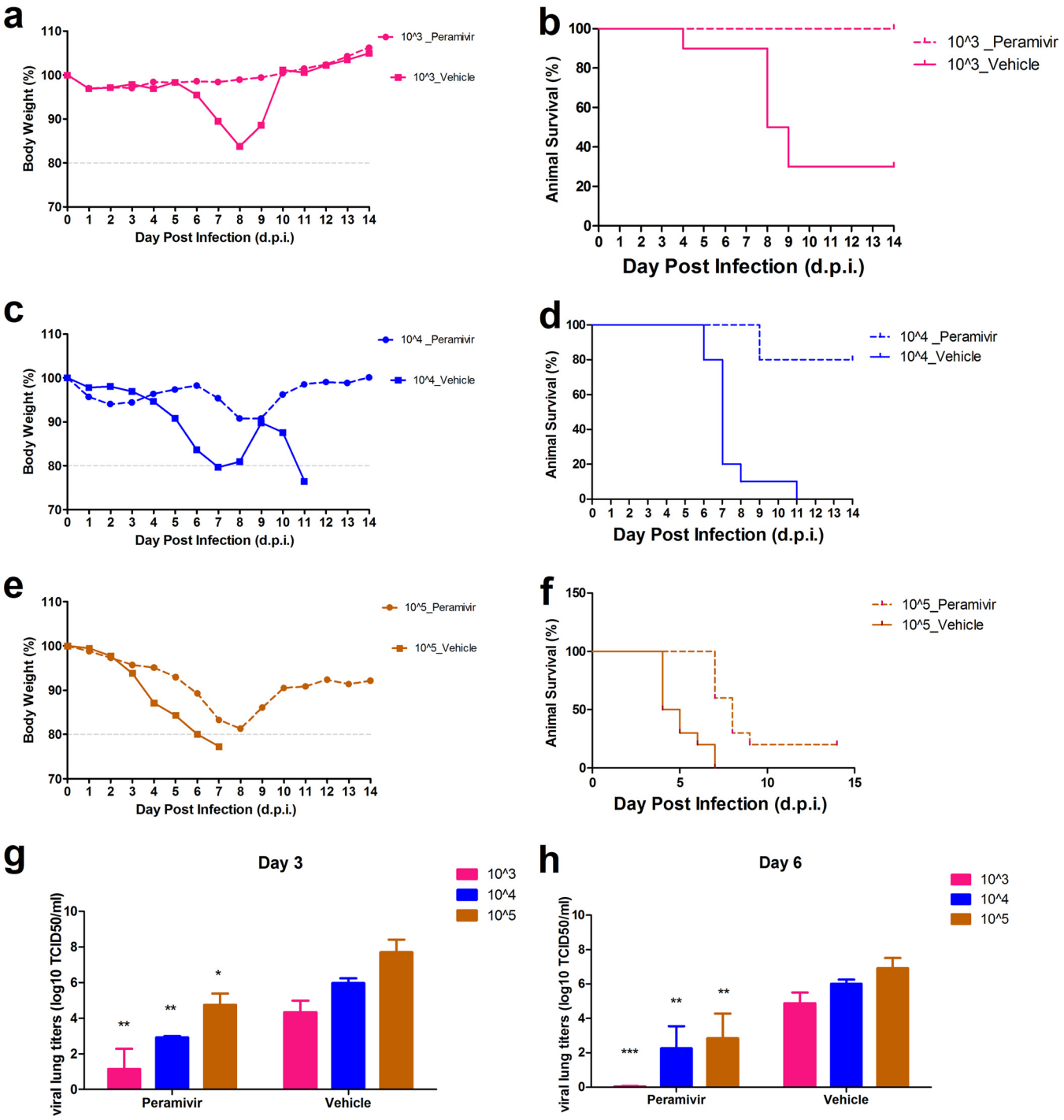

FIG 3 Peramivir mediated protection of mice against lethal H7N9 challenge. Animals were infected with the indicated viral concentrations, and 30 mg/kg of peramivir was administered intramuscularly once daily from the time of infection until 8 dpi. Significant changes in animal body weight (a, c, and e) and lethality (b, d, and f) were observed after peramivir treatment throughout the course of infection. MDCK cells were used to titrate viral loads present in lung tissues of peramivir- or vehicle (0.85% NaCl)-treated animals at 3 dpi (g) and 6 dpi (h). Results are expressed as the $\log_{10}$ mean $TCID_{50}$/ml ± standard error of the mean (SEM) for each group of mice ($n = 3$). *, $P < 0.01$; **, $P < 0.001$; ***, $P < 0.0001$.

survival benefit were observed, peramivir treatment did not bring about significant improvements in lung pathology during the acute phase of disease, such as at 3 and 6 dpi. Diffused interstitial pneumonia combined with bronchial necrosis and infiltration of mononuclear cells, comparable to that in the controls, was observed in peramivir-treated animals at 6 dpi (Fig. 4A and D). Histological analysis of surviving animals in the peramivir group revealed that by 14 dpi, most of the lung architecture was devoid of inflammatory cell infiltration, and inflamed areas were rarely observed toward the periphery (Fig. 4B). Virus-infected cells in

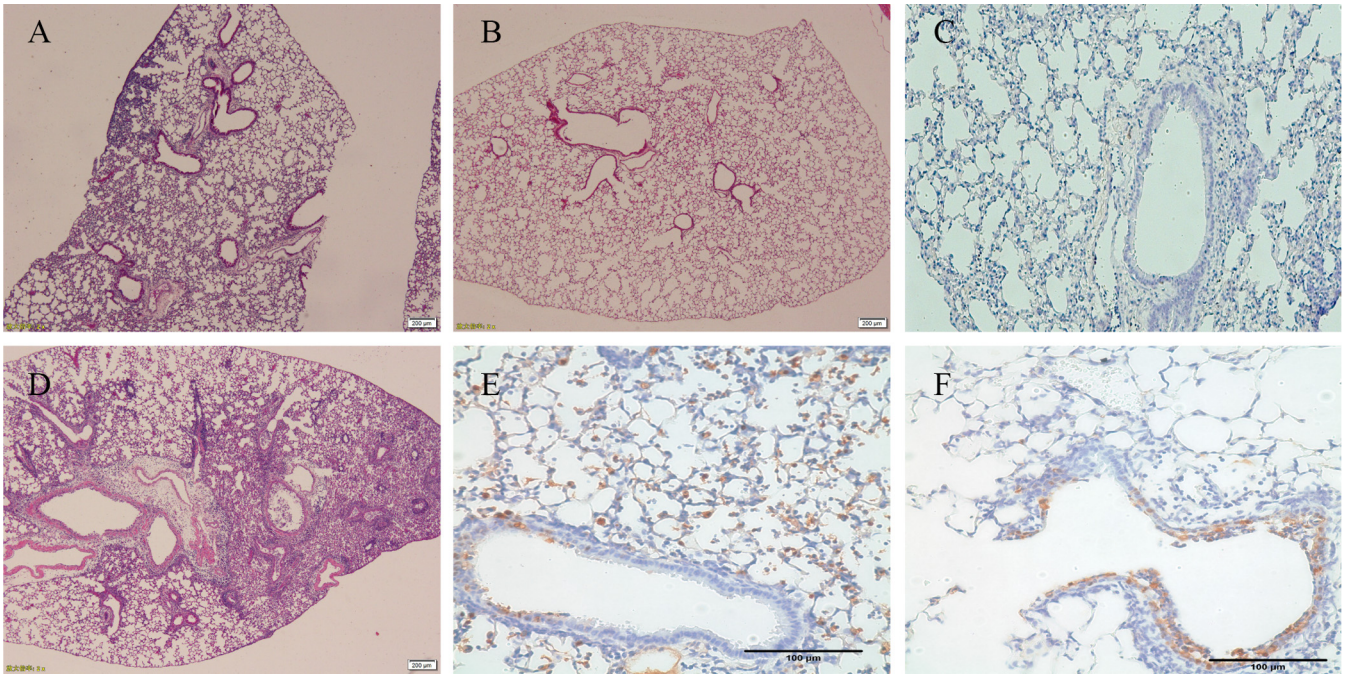

FIG 4 Temporal changes in H7N9-induced lung pathology following peramivir treatment. The images show H&E staining of lung sections. (A) Peramivir (30 mg/kg; D0 to D8)-treated animals showed minimal resolution of lung pathology compared to untreated infected animals (D) at 6 dpi. (B) Surviving animals in the peramivir-treated group showed resolved lung pathology, as evidenced by normal lung architecture in 90% of areas and localized inflammation in certain places, at 14 dpi. Lung sections stained with influenza virus NP antibody showed minimal signs of infection in peramivir-treated animals (magnification, ×100) (C), while infection of type II pneumocytes (E), inflammatory cells, and bronchial epithelium (F) was observed in untreated infected animals (magnification, ×400).

bronchial epithelium and alveolar spaces were rarely seen when lung sections of peramivir-treated animals were stained with an influenza virus nucleoprotein (NP) antibody (Fig. 4C), whereas no infected cells were found in surviving animals at 14 dpi. In contrast, vehicle-treated mice showed infection of multiple cell types, including epithelial cells from bronchi, terminal bronchioles, and the alveolar lining, where mainly type II pneumocytes were found to be infected (Fig. 4E and F). Infiltrating cells in heavily inflamed areas exhibited NP-positive staining, indicating the capability of H7N9 influenza virus to infect multiple cell types (Fig. 4F). Our findings clearly suggest that viral replication is directly correlated with an uncontrollable H7N9 influenza virus-induced lung pathology that leads to irreparable physiological damage and compromised animal health. Peramivir treatment decreased viral replication during the acute phase of infection, which subsequently helped the animals to resolve pathological signs and to regain body weight during the recovery phase.

Dose-dependent antiviral effect of peramivir on H7N9 influenza virus. To determine the therapeutic concentration of peramivir, different doses of peramivir (30, 15, and 3 mg/kg/day) were administered to separate groups of C57/BL6 mice from 0 to 8 dpi. Animals were infected with 10^4 EID_{50} of A/Shantou/1001/2014 (H7N9) virus. We found that peramivir at all doses tested improved the animal survival rate ($P < 0.0001$). Lower doses, such as 15 and 3 mg/kg, helped 30 and 20% of the animals to survive, respectively, with a delay in the median time of death from 7 to 9 dpi (Fig. 5b). The areas under the curve (AUCs) for animal weights from 1 to 14 dpi showed comparable improvements in animals after treatment with different doses; however, significant differences in weight loss were specifically observed at 5, 6, and 7 dpi ($P < 0.001$) (Fig. 5a and c). Although all doses were able to reduce viral titers in the same manner at 3 dpi ($P < 0.0001$), a dose-dependent effect was found at 6 dpi ($P < 0.001$) that might account for the beneficial effects on disease outcome (Fig. 5d).

Therapeutic effect of single versus multiple doses on H7N9 influenza virus infection. We observed that peramivir treatment from 0 to 8 dpi efficiently inhibited viral replication in the lungs and protected animals from lethal disease. Therefore, we next evaluated four different treatment regimens in infected mice. Peramivir (30 mg/kg) was administered immediately or 24 h after inoculation of mice. Peramivir treatment was given as either a single dose or multiple doses until 8 dpi (see Appendix SA2 in the supplemental material). A single dose of peramivir at the time of infection (D0 single) provided a significant improvement in weight loss, leading to protection in 50% of animals ($P < 0.0005$). In addition, the single-dose regimen substantially lowered the lung viral titer if initiated at the time of infection ($P < 0.005$). We further observed that a 24-h delayed treatment with either the single- or multiple-dose regimen significantly decreased the therapeutic capacity of peramivir. Only 20% of animals in the delayed-treatment groups were able to overcome lethal virus challenge. However, viral titers were significantly lower in lung samples from mice on the delayed multiple-dose regimen (D1 multiple) than in those from mice receiving vehicle ($P < 0.005$) (Fig. 6).

Resolution of H7N9-associated neurological symptoms and brain virus titers after peramivir treatment. Avian influenza viruses, including H5N1 and H7N9 viruses, are known for their neurovirulent characteristic in humans and animals (26–28). In

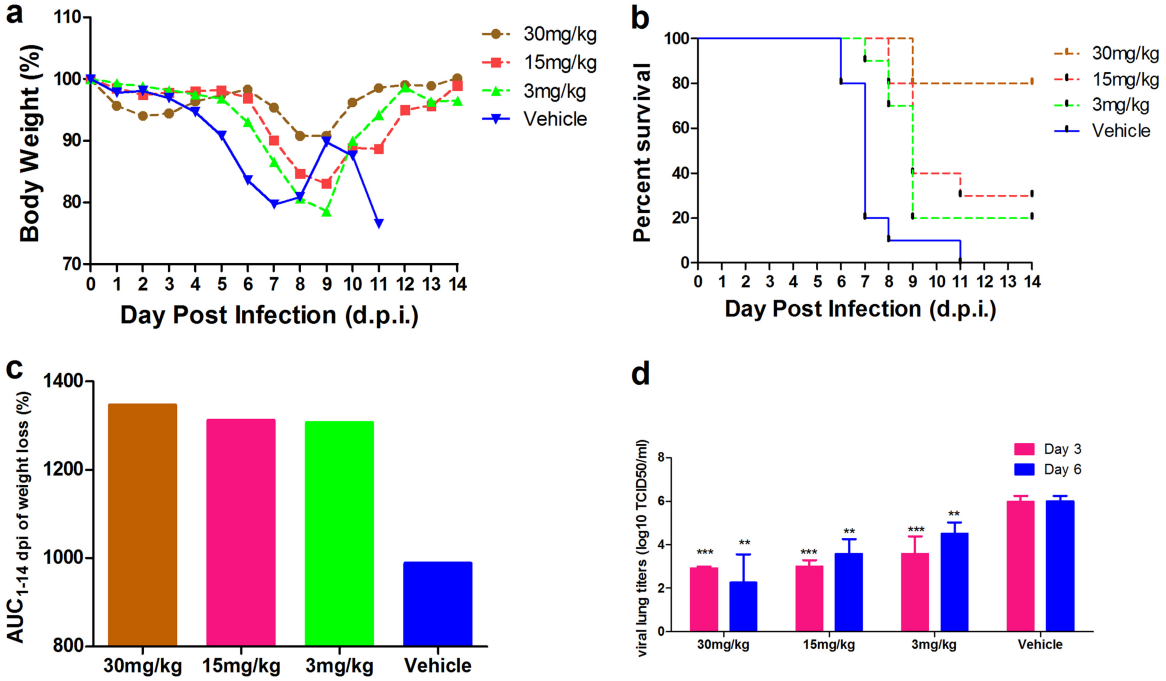

FIG 5 Dose-dependent effect of peramivir on lethal H7N9 influenza virus challenge in mice. Animals were infected with 10^4 EID_{50} of A/Shantou/1001/2014 H7N9 virus and administered 30, 15, or 3 mg/kg/day of peramivir intramuscularly from 0 to 8 dpi. Peramivir provided protection against lethal H7N9 infection in a dose-dependent manner. Changes in animal weight (a) and lethality (b) were observed throughout the course of infection. (c) The AUCs for animal weights from 1 to 14 dpi showed a 2-fold improvement for peramivir-treated animals ($n = 10$/group). (d) Dose-dependent reductions of viral loads in lung homogenates from peramivir-treated animals were seen at 3 and 6 dpi. Results are expressed as the $\log_{10}$ mean $TCID_{50}$/ml ± SEM for each group of mice ($n = 3$). ***, $P < 0.0001$; **, $P < 0.001$.

this study, we observed that A/Shantou/1001/2014 (H7N9) virus-infected animals exhibited neurological symptoms, such as tremors, hind-limb paralysis, and hunched posture. Furthermore, brain tissues of animals infected with virus at 10^5 and 10^4 EID_{50} showed high viral titers at 3 dpi. In mice treated with multiple doses of peramivir, complete inhibition of viral replication in the brain was observed at 3 dpi irrespective of the viral infective dose ($P < 0.0001$). A 1.5-$\log_{10}$ reduction in viral load was also found in animals treated with a single dose of peramivir at the time of infection ($P < 0.05$). Interestingly, peramivir treatment was also helpful for resolving H7N9-induced neurological symptoms in mice (Table 1).

Histological analysis revealed the presence of brain lesions in H7N9-infected mice at 3 and 6 dpi. Animals examined at 3 dpi had severe hemorrhaging in the frontal cortex and midbrain. Scattered foci of inflammatory cell infiltration were also observed in these regions. Signs of neural degeneration and liquefaction were seen in the cerebral cortex at 3 dpi and led to karyopyknosis at 6 dpi. Furthermore, inflammation of the meninges was seen, with infiltrating cells, neural edema in the frontal cortex, and an increased size of the arachnoid space. In peramivir-treated animals, signs of hemorrhage were minimal compared to those in the untreated group; however, there were foci of infiltrating cells and neural degeneration (Fig. 7).

DISCUSSION

Here we present a mouse model of H7N9 influenza virus infection that can be used to assess the therapeutic potential of antiviral

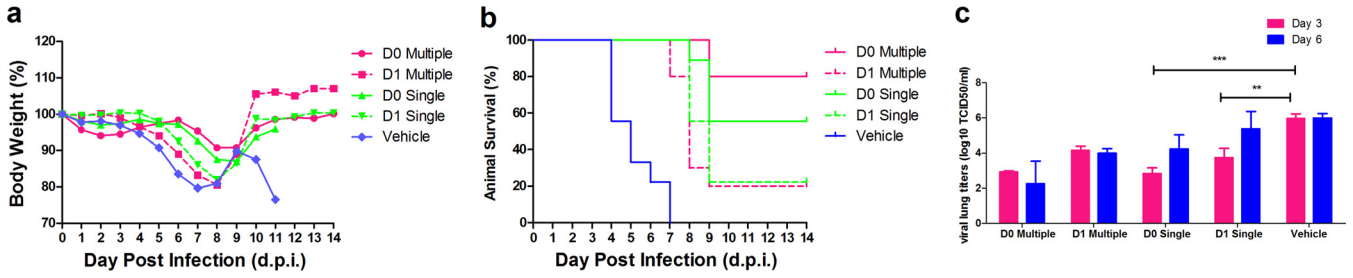

FIG 6 Comparison of single and multiple doses of peramivir. Animals were infected with 10^4 EID_{50} of A/Shantou/1001/2014 H7N9 virus. Single-dose regimens consisted of 30 mg/kg/day of peramivir administered intramuscularly at the time of infection (D0 single) or at 1 dpi (D1 single). In multiple-dose regimens, similar peramivir treatments were initiated either at the time of infection (D0 multiple) or at 1 dpi (D1 multiple) and continued until 8 dpi. Changes in animal weight (a) and lethality (b) were observed throughout the course of infection. (c) Reductions of viral loads in lung homogenates from peramivir-treated animals were seen at 3 and 6 dpi. Results are expressed as the $\log_{10}$ mean $TCID_{50}$/ml ± SEM for each group of mice ($n = 3$). ***, $P < 0.0005$; **, $P < 0.005$.

TABLE 1 Resolution of neurological signs in H7N9-infected animals after peramivir treatment[a]

Infective dose (EID_{50})	Treatment	No. of animals with neurological signs/total no. of animals	Viral copy number/ml of brain homogenate at 3 dpi ($n = 3$/group)	Neurological sign(s)
10^4	30 mg/kg peramivir, multiple doses (D0 to D8)	0/10	0	
	30 mg/kg peramivir, single dose	0/10	1.52E+03	
	Vehicle	1/10	3.55E+04	Hind-limb paralysis
10^5	30 mg/kg peramivir, multiple doses (D0 to D8)	4/10	0	Tremors, hunched posture
	Vehicle	8/10	1.50E+03	Tremors, hunched posture, minimal activity

[a] The EID_{50} is the concentration of virus that can infect 50% of inoculated eggs. Viral copy numbers were determined by performing qRT-PCR on RNAs extracted from brain tissue homogenates.

drugs. We found that A/Shantou/1001/2014 (H7N9) virus, which was isolated from a fatal human case during the second wave of the epidemic, efficiently replicated in the respiratory tract, induced interstitial pneumonia and inflammatory cell infiltration in the lungs, and caused lethal infection in mice even at the lowest challenge dose (10^3 EID_{50}). The virus was able to disseminate to extrapulmonary tissues, indicating the efficiency of the mouse model for replicating the vital properties of H7N9 infection in humans. A/Shantou/1001/2014 (H7N9) virus belongs to the major phylogenetic group of H7N9 viruses that were widely distributed across China during the first and second waves of the H7N9 flu epidemic (25). Previous studies showed inconsistency in the pathogenicities of ancestral H7N9 strains in mice. The A/Anhui/1/2013 (H7N9) and A/Shanghai/1/2013 (H7N9) viruses were found to be lethal, with a 50% lethal dose in mice (MLD_{50}) of $10^{3.5}$ PFU (29, 30), but no lethal infection was seen by Mok et al. (31) in mice infected with higher doses of A/Shanghai/2/2013 (H7N9) virus. Signature amino acid mutations, specifically those in hemagglutinin (HA) and the polymerase complex that are linked to adaptation to the mammalian host and to viral replication efficiency, have been attributed to various pathogenicity profiles of H7N9 influenza viruses. For instance, the Q226L mutation in the HA gene, associated with increased binding to mammalian receptors, is found in some H7N9 strains (29). In addition, the PB2 E627K mutation, which is known to aid in avian virus adaptation to mammalian hosts, is also present in H7N9 strains isolated from humans (32). A/Shantou/1001/2014 (H7N9) virus contains both these mutations (25), like its early ancestors, which explains its pathogenic potential and high replication tendency in the mammalian environment.

Continuous evolution of newly emerged H7N9 influenza viruses has increased the risk of infecting populations on a larger scale. Severe human H7N9 cases are currently being treated with NAIs. Among the NAIs, only oseltamivir has been tested for anti-H7N9 influenza virus activity in animals (18, 33). The present study demonstrates for the first time the antiviral activity of peramivir against an H7N9 virus in mice. Peramivir is known to be administered intravenously, particularly to patients who develop severe influenza virus infections. However, clinical efficacy trials were performed on intravenous as well as intramuscular administration of peramivir, and the results showed the superior efficacy of these routes over oral administration to patients with complicated and uncomplicated influenza virus infections (34). The drug has a higher affinity for binding to the neuraminidase enzyme (35) and also achieves a longer plasma elimination half-life (36) if administered by the intravenous and intramuscular routes. However, most animal studies have been performed by the intravenous route of administration, except for a few that showed successful antiviral therapies by the intramuscular route (37, 38). Considering that intramuscular injections are easily achievable and less time-consuming in small animals, with no inferior efficacy, a rationale was made to use this route in this study.

Our studies showed that repeated administration of 30 mg/kg peramivir starting from the day of infection until 8 dpi is capable of protecting animals against lethal H7N9 influenza virus infection. This protection may be the result of successful viral eradication from the lungs by 3 and 6 dpi, indicating direct antiviral effects of peramivir that reduce pathology toward the end of the disease course. In addition, peramivir treatment greatly affected the biodistribution of H7N9 virus in various extrapulmonary tissues.

The H7N9 virus is known to cause a severe form of disease in humans, with increased mortalities during the second and third waves of the epidemic (39). Patients with this severe disease require aggressive treatment and mechanical ventilation and stay longer in hospitals (40, 41). Moreover, clinical studies have shown the tendency of H7N9-infected patients to shed virus into the respiratory tract for long periods, which subsequently affects the clinical outcome of disease (24). The situation indicates that patients with severe cases need to have a longer duration of antiviral treatment. In this context, we decided to assess a longer treatment regimen that consisted of nine consecutive doses of peramivir, starting either at the time of infection of animals or a day after. The 24-h delay in drug administration showed readily apparent differences between the two regimens. As shown by observational studies performed with pandemic H1N1 human cases (21, 42), delayed treatment of peramivir in H7N9-infected animals remained sufficient enough to eradicate the virus but resulted in moderate effects on the disease process. Our further experiment assessing the effects of single- and multiple-dose regimens also confirmed that the time for the initiation of treatment is critical to obtain a survival benefit. A single dose of peramivir administered on the day of infection provided greater clinical benefits to the animals than the multiple-dose regimen initiated with a delay of 24 h.

Neurovirulence is one of the vital properties of some influenza viruses, such as H1N1 and H5N1, and this is considered a contributing factor in several neurodegenerative diseases (43, 44). Previous studies have defined that influenza virus infection of neural cells can induce encephalitis directly (45–47). The neurovirulence of H7N9 is a matter of great concern. Clinical studies reported the

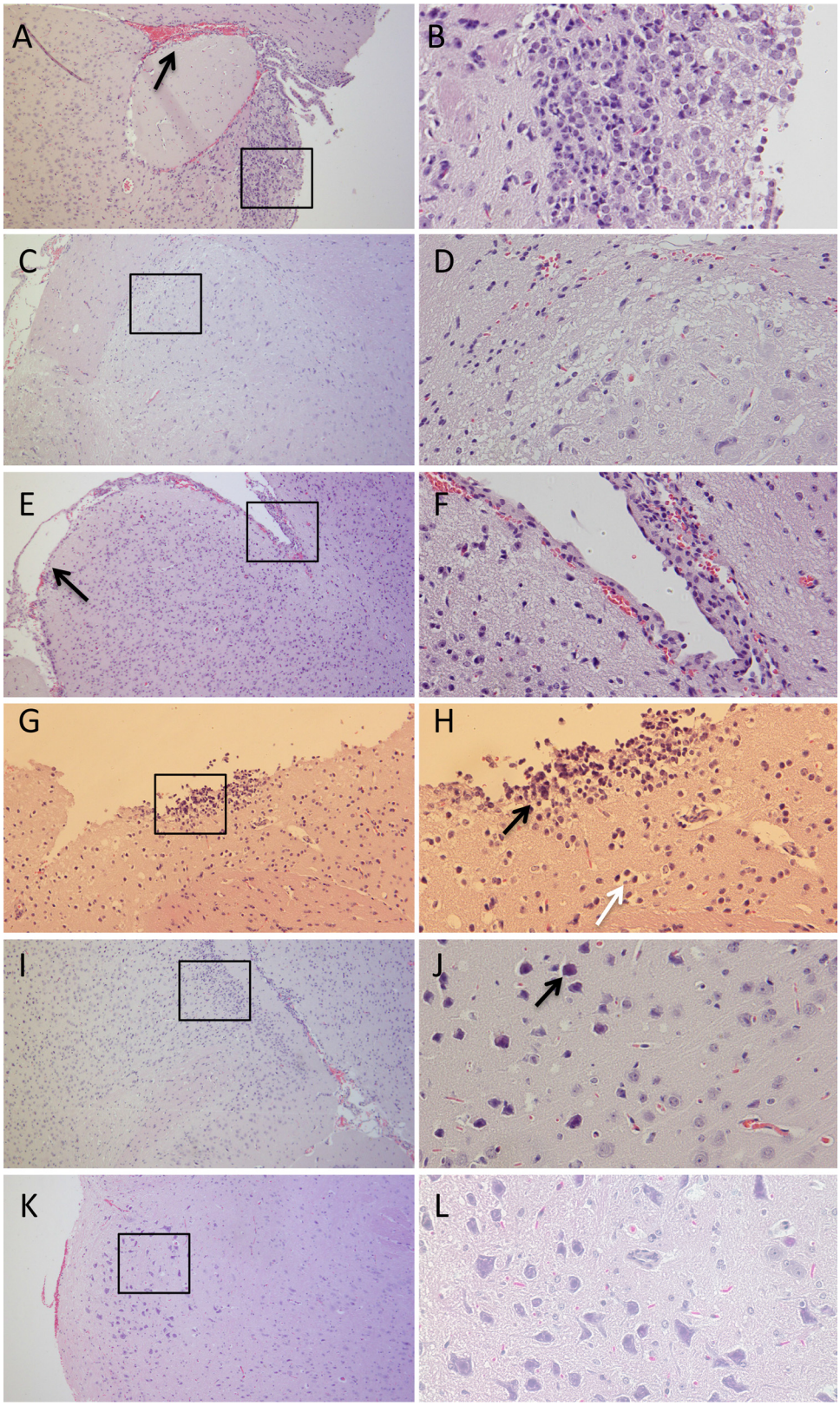

FIG 7 Pathological changes in brain tissues after A/Shantou/1001/2014 (H7N9) infection in C57/BL6 mice. Representative sections show hemorrhaging (black arrow) (A), degenerative neurons and infiltrating cells (B), liquefaction of neural cells in the midbrain (C and D), an increased size of the arachnoid space (E), and hemorrhaging in the cerebral cortex (E and F). (G and H) Infiltration of inflammatory cells (black arrow) and neural edema (white arrow) in the frontal cortex at 3 dpi. (I and J) Karyopyknosis (black arrow) in the cerebrum at 6 dpi. (K and L) Minimal signs of hemorrhage associated with neural degeneration in H7N9-infected animals after treatment with 30 mg/kg of peramivir at 3 dpi. Left panels show higher-magnification (×400) views of the boxes in the right panels.

possible involvement of the brain in severe cases of H7N9 infection (4, 48). In addition, we previously observed H7N9 viral infection in brain tissues from ferrets, but none of these animals exhibited neurological signs (10). This study confirms that H7N9 influenza virus is neurovirulent in mice, as the virus was found in brain tissues and the animals exhibited a variety of neurological symptoms and brain lesions. Interestingly, single and multiple peramivir administrations were capable of eradicating virus from the brain, preventing neurological signs from occurring. This study clearly indicates that, as in the H5N1 infection model, the clinical benefits of peramivir are not limited to localized virus infection in the respiratory tract (49).

The rapid bioavailability of intravenous or intramuscular peramivir aids in the superior clinical efficacy of this drug administered by these routes over oral administration. For H1N1 and other influenza viruses, the drug has been tested in controlled trials of prophylaxis and treatment. These studies provide strong evidence for a direct relationship to virus eradication and earlier relief of influenza-like illness (ILI) (22, 50). The present study provides the first evidence of antiviral activity of peramivir toward H7N9 viruses. Antiviral treatment contributed to the resolution of clinical signs, increased survival, and prevented the occurrence of neurological symptoms in mice. This suggests that rapid assessment of the clinical efficacy of this drug is urgently required for its possible use as a treatment option for future severely H7N9-infected individuals.

ACKNOWLEDGMENTS

We thank the technical and nontechnical staff of the Division of Immunology, International Institute of Infection and Immunity, for their help.

This study was supported by a grant from the Li Ka Shing Foundation.

REFERENCES

1. **Guan Y, Farooqui A, Zhu H, Dong W, Wang J, Kelvin DJ.** 2013. H7N9 incident, immune status, the elderly and a warning of an influenza pandemic. J Infect Dev Ctries **7:**302–307. http://dx.doi.org/10.3855/jidc.3675.
2. **Chen E, Chen Y, Fu L, Chen Z, Gong Z, Mao H, Wang D, Ni M, Wu P, Yu Z, He T, Li Z, Gao J, Liu S, Shu Y, Cowling BJ, Xia S, Yu H.** 2013. Human infection with avian influenza A (H7N9) virus re-emerges in China in winter 2013. Euro Surveill **18:**20616.
3. **WHO.** 2015. Human infection with avian influenza A(H7N9) virus—China. World Health Organization, Geneva, Switzerland.
4. **Gao H-N, Lu H-Z, Cao B, Du B, Shang H, Gan J-H, LuS-H, Yang Y-D, Fang Q, Shen Y-Z.** 2013. Clinical findings in 111 cases of influenza A (H7N9) virus infection. N Engl J Med **368:**2277–2285. http://dx.doi.org/10.1056/NEJMoa1305584.
5. **China Health and Family Planning Commission.** 2015. National statutory infectious diseases overview. China Health and Family Planning Commission, Beijing, China.
6. **Center for Health Protection.** 2015. Avian influenza report, reporting period: February 1, 2015–February 7, 2015 (week 6). Center for Health Protection, Department of Health, Hong Kong Special Administrative Region.
7. **Chang S-Y, Lin P-H, Tsai J-C, Hung C-C, Chang S-C.** 2013. The first case of H7N9 influenza in Taiwan. Lancet **381:**1621. http://dx.doi.org/10.1016/S0140-6736(13)60943-5.
8. **Public Health Agency of Canada.** 2015. Government of Canada and British Columbia confirm case of H7N9 avian influenza in Canada. Public Health Agency of Canada, Government of Canada, Vancouver, Canada.
9. **Rosen JB, Rota JS, Hickman CJ, Sowers SB, Mercader S, Rota PA, Bellini WJ, Huang AJ, Doll MK, Zucker JR, Zimmerman CM.** 2014. Outbreak of measles among persons with prior evidence of immunity, New York City, 2011. Clin Infect Dis **58:**1205–1210. http://dx.doi.org/10.1093/cid/ciu105.
10. **Zhu H, Wang D, Kelvin D, Li L, Zheng Z, Yoon S-W, Wong S-S, Farooqui A, Wang J, Banner D, Chen R, Zheng R, Zhou J, Zhang Y, Hong W, Dong W, Cai Q, Roehrl MH, Huang SS, Kelvin AA, Yao T, Zhou B, Chen X, Leung GM, Poon LL, Webster RG, Webby RJ, Peiris JS, Guan Y, Shu Y.** 2013. Infectivity, transmission, and pathology of human-isolated H7N9 influenza virus in ferrets and pigs. Science **341:**183–186. http://dx.doi.org/10.1126/science.1239844.
11. **Qi X, Qian Y-H, Bao C-J, Guo X-L, Cui L-B, Tang F-Y, Ji H, Huang Y, Cai P-Q, Lu B, Xu K, Shi C, Zhu FC, Zhou MH, Wang H.** 2013. Probable person to person transmission of novel avian influenza A (H7N9) virus in eastern China, 2013: epidemiological investigation. BMJ **347:**f4752. http://dx.doi.org/10.1136/bmj.f4752.
12. **Hay AJ, Hayden FG.** 2013. Oseltamivir resistance during treatment of H7N9 infection. Lancet **381:**2230–2232. http://dx.doi.org/10.1016/S0140-6736(13)61209-X.
13. **Hai R, Schmolke M, Leyva-Grado VH, Thangavel RR, Margine I, Jaffe EL, Krammer F, Solórzano A, García-Sastre A, Palese P, Bouvier NM.** 2013. Influenza A (H7N9) virus gains neuraminidase inhibitor resistance without loss of in vivo virulence or transmissibility. Nat Commun **4:**2854. http://dx.doi.org/10.1038/ncomms3854.
14. **Leung YH, To MK, Lam TS, Yau SW, Leung OS, Chuang SK.** 2015. Epidemiology of human influenza A(H7N9) infection in Hong Kong. J Microbiol Immunol Infect **2015:**S1684–1182(15)00772-0. http://dx.doi.org/10.1016/j.jmii.2015.06.004.
15. **Li Q, Zhou L, Zhou M, Chen Z, Li F, Wu H, Xiang N, Chen E, Tang F, Wang D.** 2014. Epidemiology of human infections with avian influenza A (H7N9) virus in China. N Engl J Med **370:**520–532. http://dx.doi.org/10.1056/NEJMoa1304617.
16. **Liu X, Li T, Zheng Y, Wong KW, Lu S, Lu H.** 2013. Poor responses to oseltamivir treatment in a patient with influenza A (H7N9) virus infection. Emerg Microbes Infect **2:**e27. http://dx.doi.org/10.1038/emi.2013.30.
17. **China Health and Family Planning Commission.** 2014. H7N9 influenza in humans; a treatment plan (2014). China Health and Family Planning Commission, Beijing, China.
18. **Baranovich T, Burnham AJ, Marathe BM, Armstrong J, Guan Y, Shu Y, Peiris JM, Webby RJ, Webster RG, Govorkova EA.** 2014. The neuraminidase inhibitor oseltamivir is effective against A/Anhui/1/2013 (H7N9) influenza virus in a mouse model of acute respiratory distress syndrome. J Infect Dis **209:**1343–1353. http://dx.doi.org/10.1093/infdis/jit554.
19. **Cao R-Y, Xiao J-H, Cao B, Li S, Kumaki Y, Zhong W.** 2014. Inhibition of novel reassortant avian influenza H7N9 virus infection in vitro with three antiviral drugs, oseltamivir, peramivir and favipiravir. Antivir Chem Chemother **23:**237–240. http://dx.doi.org/10.3851/IMP2672.
20. **Birnkrant D, Cox E.** 2009. The emergency use authorization of peramivir for treatment of 2009 H1N1 influenza. N Engl J Med **361:**2204–2207. http://dx.doi.org/10.1056/NEJMp0910479.
21. **Hernandez JE, Adiga R, Armstrong R, Bazan J, Bonilla H, Bradley J, Dretler R, Ison MG, Mangino JE, Maroushek S.** 2011. Clinical experience in adults and children treated with intravenous peramivir for 2009 influenza A (H1N1) under an emergency IND program in the United States. Clin Infect Dis **52:**695–706. http://dx.doi.org/10.1093/cid/cir001.
22. **Kohno S, Kida H, Mizuguchi M, Hirotsu N, Ishida T, Kadota J, Shimada J.** 2011. Intravenous peramivir for treatment of influenza A and B virus infection in high-risk patients. Antimicrob Agents Chemother **55:**2803–2812. http://dx.doi.org/10.1128/AAC.01718-10.
23. **Shobugawa Y, Saito R, Sato I, Kawashima T, Dapat C, Dapat IC, Kondo H, Suzuki Y, Saito K, Suzuki H.** 2012. Clinical effectiveness of neuraminidase inhibitors— oseltamivir, zanamivir, laninamivir, and peramivir—for treatment of influenza A (H3N2) and A (H1N1) pdm09 infection: an observational study in the 2010–2011 influenza season in Japan. J Infect Chemother **18:**858–864. http://dx.doi.org/10.1007/s10156-012-0428-1.
24. **Hu Y, Lu S, Song Z, Wang W, Hao P, Li J, Zhang X, Yen H-L, Shi B, Li T, Guan W, Xu L, Liu Y, Wang S, Zhang X, Tian D, Zhu Z, He J, Huang K, Chen H, Zheng L, Li X, Ping J, Kang B, Xi X, Zha L, Li Y, Zhang Z, Peiris M, Yuan Z.** 2013. Association between adverse clinical outcome in human disease caused by novel influenza A H7N9 virus and sustained viral shedding and emergence of antiviral resistance. Lancet **381:**2273–2279. http://dx.doi.org/10.1016/S0140-6736(13)61125-3.
25. **Farooqui A, Leon AJ, Huang L, Wu S, Cai Y, Lin P, Chen W, Fang X, Zeng T, Liu Y.** 2015. Genetic diversity of the 2013–14 human isolates of influenza H7N9 in China. BMC Infect Dis **15:**109. http://dx.doi.org/10.1186/s12879-015-0829-8.
26. **Gao R, Cao B, Hu Y, Feng Z, Wang D, Hu W, Chen J, Jie Z, Qiu H, Xu K.** 2013. Human infection with a novel avian-origin influenza A

(H7N9) virus. N Engl J Med **368:**1888–1897. http://dx.doi.org/10.1056/NEJMoa1304459.
27. **Lipatov AS, Krauss S, Guan Y, Peiris M, Rehg JE, Perez DR, Webster RG.** 2003. Neurovirulence in mice of H5N1 influenza virus genotypes isolated from Hong Kong poultry in 2001. J Virol **77:**3816–3823. http://dx.doi.org/10.1128/JVI.77.6.3816-3823.2003.
28. **Plourde JR, Pyles JA, Layton RC, Vaughan SE, Tipper JL, Harrod KS.** 2012. Neurovirulence of H5N1 infection in ferrets is mediated by multifocal replication in distinct permissive neuronal cell regions. PLoS One **7:**e46605. http://dx.doi.org/10.1371/journal.pone.0046605.
29. **Belser JA, Gustin KM, Pearce MB, Maines TR, Zeng H, Pappas C, Sun X, Carney PJ, Villanueva JM, Stevens J, Katz JM, Tumpey TM.** 2013. Pathogenesis and transmission of avian influenza A (H7N9) virus in ferrets and mice. Nature **501:**556–559. http://dx.doi.org/10.1038/nature12391.
30. **Watanabe T, Kiso M, Fukuyama S, Nakajima N, Imai M, Yamada S, Murakami S, Yamayoshi S, Iwatsuki-Horimoto K, Sakoda Y, Takashita E, McBride R, Noda T, Hatta M, Imai H, Zhao D, Kishida N, Shirakura M, de Vries RP, Shichinohe S, Okamatsu M, Tamura T, Tomita Y, Fujimoto N, Goto K, Katsura H, Kawakami E, Ishikawa I, Watanabe S, Ito M, Sakai-Tagawa Y, Sugita Y, Uraki R, Yamaji R, Eisfeld AJ, Zhong G, Fan S, Ping J, Maher EA, Hanson A, Uchida Y, Saito T, Ozawa M, Neumann G, Kida H, Odagiri T, Paulson JC, Hasegawa H, Tashiro M, Kawaoka Y.** 2013. Characterization of H7N9 influenza A viruses isolated from humans. Nature **501:**551–555. http://dx.doi.org/10.1038/nature12392.
31. **Mok CKP, Lee HHY, Chan MCW, Sia SF, Lestra M, Nicholls JM, Zhu H, Guan Y, Peiris JMS.** 2013. Pathogenicity of the novel A/H7N9 influenza virus in mice. mBio **4:**e00362-13. http://dx.doi.org/10.1128/mBio.00362-13.
32. **Zhang H, Li X, Guo J, Li L, Chang C, Li Y, Bian C, Xu K, Chen H, Sun B.** 2014. The PB2 E627K mutation contributes to the high polymerase activity and enhanced replication of H7N9 influenza virus. J Gen Virol **95:**779–786. http://dx.doi.org/10.1099/vir.0.061721-0.
33. **Marjuki H, Mishin VP, Chesnokov AP, Juan A, Fry AM, Villanueva J, Gubareva LV.** 2014. An investigational antiviral drug, DAS181, effectively inhibits replication of zoonotic influenza A virus subtype H7N9 and protects mice from lethality. J Infect Dis **210:**435–440. http://dx.doi.org/10.1093/infdis/jiu105.
34. **Whitley R, Laughlin A, Carson S, Mitha E, Tellier G, Stich M, Elder J, Alexander WJ, Dobo S, Collis P, Sheridan WP.** 15 October 2014. Single dose peramivir for the treatment of acute seasonal influenza: integrated analysis of efficacy and safety from two placebo-controlled trials. Antivir Ther http://dx.doi.org/10.3851/IMP2874.
35. **Bantia S, Upshaw R, Babu Y.** 2011. Characterization of the binding affinities of peramivir and oseltamivir carboxylate to the neuraminidase enzyme. Antiviral Res **91:**288–291. http://dx.doi.org/10.1016/j.antiviral.2011.06.010.
36. **Hayden F.** 2009. Developing new antiviral agents for influenza treatment: what does the future hold? Clin Infect Dis **48:**S3–S13. http://dx.doi.org/10.1086/591851.
37. **Abed Y, Pizzorno A, Boivin G.** 2012. Therapeutic activity of intramuscular peramivir in mice infected with a recombinant influenza A/WSN/33 (H1N1) virus containing the H275Y neuraminidase mutation. Antimicrob Agents Chemother **56:**4375–4380. http://dx.doi.org/10.1128/AAC.00753-12.
38. **Bantia S, Arnold CS, Parker CD, Upshaw R, Chand P.** 2006. Anti-influenza virus activity of peramivir in mice with single intramuscular injection. Antiviral Res **69:**39–45. http://dx.doi.org/10.1016/j.antiviral.2005.10.002.
39. **Feng L, Wu J, Liu X, Yang P, Tsang T, Jiang H, Wu P, Yang J, Fang V, Qin Y, Lau EH, Li M, Zheng J, Peng Z, Xie Y, Wang Q, Li Z, Leung GM, Gao GF, Yu H, Cowling BJ.** 2014. Clinical severity of human infections with avian influenza A (H7N9) virus, China, 2013/14. Euro Surveill **19:**20984.
40. **Tang X, He H, Sun B, Wan J, Ban C, Zhang C, Wang S, Xia J, Li J, Liu Y, Cao B, Tong Z.** 2015. ARDS associated with pneumonia caused by avian influenza A H7N9 virus treated with extracorporeal membrane oxygenation. Clin Respir J **9:**380–384. http://dx.doi.org/10.1111/crj.12140.
41. **Yu H, Cowling BJ, Feng L, Lau EH, Liao Q, Tsang TK, Peng Z, Wu P, Liu F, Fang VJ.** 2013. Human infection with avian influenza A H7N9 virus: an assessment of clinical severity. Lancet **382:**138–145. http://dx.doi.org/10.1016/S0140-6736(13)61207-6.
42. **Uyeki T.** 2009. Antiviral treatment for patients hospitalized with 2009 pandemic influenza A (H1N1). N Engl J Med **361:**e110. http://dx.doi.org/10.1056/NEJMopv0910738.
43. **Jang H, Boltz D, Sturm-Ramirez K, Shepherd KR, Jiao Y, Webster R, Smeyne RJ.** 2009. Highly pathogenic H5N1 influenza virus can enter the central nervous system and induce neuroinflammation and neurodegeneration. Proc Natl Acad Sci U S A **106:**14063–14068. http://dx.doi.org/10.1073/pnas.0900096106.
44. **Li S, Schulman J, Itamura S, Palese P.** 1993. Glycosylation of neuraminidase determines the neurovirulence of influenza A/WSN/33 virus. J Virol **67:**6667–6673.
45. **Drago L, Attia MW, DePiero A, Bean C.** 2005. Influenza A-associated meningoencephalitis. Pediatr Emerg Care **21:**437–439. http://dx.doi.org/10.1097/01.pec.0000169434.98819.05.
46. **Hayase Y, Tobita K.** 1997. Influenza virus and neurological diseases. Psychiatry Clin Neurosci **51:**181–184. http://dx.doi.org/10.1111/j.1440-1819.1997.tb02580.x.
47. **Togashi T, Matsuzono Y, Narita M, Morishima T.** 2004. Influenza-associated acute encephalopathy in Japanese children in 1994–2002. Virus Res **103:**75–78. http://dx.doi.org/10.1016/j.virusres.2004.02.016.
48. **Lu S, Xi X, Zheng Y, Cao Y, Liu X, Lu H.** 2013. Analysis of the clinical characteristics and treatment of two patients with avian influenza virus (H7N9). Biosci Trends **7:**109–112.
49. **Yun NE, Linde NS, Zacks MA, Barr IG, Hurt AC, Smith JN, Dziuba N, Holbrook MR, Zhang L, Kilpatrick JM.** 2008. Injectable peramivir mitigates disease and promotes survival in ferrets and mice infected with the highly virulent influenza virus, A/Vietnam/1203/04 (H5N1). Virology **374:**198–209. http://dx.doi.org/10.1016/j.virol.2007.12.029.
50. **Barroso L, Treanor J, Gubareva L, Hayden FG.** 2005. Efficacy and tolerability of the oral neuraminidase inhibitor peramivir in experimental human influenza: randomized, controlled trials for prophylaxis and treatment. Antiviral Ther **10:**901–910.